Starchy plastic

by

Rovan Ashraf, Ahmed Weal, Mohamed Adel, Omar Mustafa

Pyramid team

#beapriate challenge 2022

Abstract

Microbial treatment of biodegradable wastes not only assures the neutralization of dangerous components such as volatile organic compounds but also allows for societal valorization and bio-circularity. Single-cell protein (SCP) is a value-added product generated through microbial fermentation from biodegradable waste sources such as food waste. SCP produced from potato starch waste was shown to be a feasible alternative to existing plant/animal proteins utilized in the manufacturing of films for purposes such as packaging in this article. Compression molding was used to make flexible glycerol-plasticized SCP films, and tensile testing demonstrated strength and stiffness comparable to other plasticized protein films. The oxygen barrier qualities were substantially better than those of typical polyethylene packaging material, however, the SCP material, like other highly polar materials, must be protected from moisture if used in food packaging, for example. The biodegradation test revealed a degradation pattern that was like that of a biodegradable bag used in the home. The findings suggest that SCP-based bioplastic films could be a viable alternative to existing plant/animal protein films and synthetic polymers.

KEYWORDS: single-cell protein, protein, bioplastic biopolymer, films

Synopsis

Flexible bioplastic sheets made from single cells are a safe and sustainable alternative to petroleum-based plastics in packaging applications.

Introduction

Because of their easy film-forming capabilities and biodegradability, proteins from plant/animal products have been in the spotlight as renewable raw materials for non-food applications, particularly food packaging. (1,2) Proteins are heteropolymer chains comprising various amino acids, unlike other bio-sourced homopolymeric polymers (e.g., polysaccharides like cellulose). This gives interactions involved in the generation of -helices, -sheets, and -turn conformations in proteins a wide range of chemical functions. (3) These interactions are what cause proteins to form films, which is why they've been employed to make bioplastic films and coatings. (5) Plant [wheat gluten (WG), soy, pea, maize zein, cottonseed protein, and so on] and animal (whey, casein, collagen, gelatin, keratin, fish myofibrillar protein, and so on) proteins are used to make today's protein-based bioplastics. However, because they compete for arable land and freshwater, some of these do not fully comply with the UN's sustainable development goals. As a result, greater reliance on plant and animal proteins for bioplastic

manufacturing soon could put significant strain on the high protein value food supply chain. This fact is exacerbated by the fact that the global population is predicted to reach 9 to 10 billion people by 2050, necessitating new and safe feeding practices. (9,10) Single-cell proteins (SCPs), which have already been used safely as feed/food, could be employed as next-generation bioplastics. The SCP is a novel proteinaceous source derived from dead and dried unicellular microbial biomass such as bacteria, fungus, and algae cultivated on agricultural wastes and industrial byproducts. (11−13) Bacterial SCP is discovered to have a high protein content and contains all the essential amino acids among the diverse species. (14,15) Protein accounts for 60–80% of the total dry weight of the cell, whereas carbs, lipids, vitamins, and minerals account for the remaining dry weight. The following are the advantages or benefits of the SCP over plant/animal proteins: (1) Because bacteria grow faster than plants and animals, they can outgrow their protein output, resulting in a surplus protein supply that can be used for non-food purposes such as the creation of safe bioplastics. In comparison to soy production of just 3 tones hectare–1 year–1 using renewable hydrogen, using solar energy (average solar radiance of 1800 kW h m–2 year–1 would deliver an equivalent of 5.6 kg H2 m–2 year–1 via photovoltaic conversion) and wind energy (2 W m–2 would deliver about 1300 kg H2 m–2year–1) to support SCP production would yield up to 67 and 3120 tones hectare–1 year–1 (16,17) (2) because the manufacture is based on external microbe cultivation. (2) Because the process relies on the external cultivation of microorganisms on plant and animal waste products, it does not require a lot of land or water, and hence does not have the same environmental and water impact as conventional agriculture. (18) (3) Unlike conventional agriculture, which uses industrially manufactured nitrogen-based fertilizers, SCP production has no carbon footprint (the Haber–Bosch process produces 4–8 tons of CO2 equivalent per ton of N fertilizer produced). Moreover, nitrate losses from agricultural land cause eutrophication and N2O greenhouse gas emissions, wreaking havoc on the environment, whereas the utilized reactive nitrogen from plant and animal wastes, as well as the released CO2, can be used as N and C sources. The development of SCP-based plastic films, such as packaging applications and other plastic goods, is reported in this article to develop not only an environmentally acceptable alternative to petroleum-based plastics but also a material that does not compete with food production. With glycerol as the plasticizer, a series of SCP-based films were made utilizing the compression molding technique at three different temperatures and compression durations. Compression molding is advantageous since it is simple to use and allows for large-scale production without the use of organic solvents for polymer solubilization. (27−31) Glycerol is a substantial byproduct of biodiesel manufacturing, and its use here is consistent with resource sustainability. better understand the behavior of protein films under various processing settings, a systematic comparative analysis of the films' thermal, mechanical, water vapor, and oxygen transmission properties was conducted.

2. Materials and methods

2.1Discussion

The SCP was produced using the potato starch present in cutting waters, which otherwise goes to the water treatment plant (Figure S1, Supporting Information). The upgrading technology is a patented aerobic fermentation process using a mixed microbiome. (32) The main components of the SCP were 66 wt % protein (Nx6.25, Kjeldahl method, 6.3 wt % total fat (gravimetric method, ISO 1443), 12.5 wt % carbohydrates [estimated by the following formula: carbohydrates = 100% – (%

ash) – (% total fat) – (% moisture) – (% Protein)], 9.5 wt % ash (ISO 946), and 5.7 wt % moisture (EG 20/12/1971 L279/8/11). Glycerol (99%) The materials were used as received.

2.2 Preparation of SCP/Glycerol Bioplastic Films

Protein films were fabricated using the compression molding technique. The flaky protein sample (Figure S1) was first ground to make a powder using a mortar and pestle. 30 wt % glycerol was added (30/70 w/w glycerol/SCP) to the powder, which was subsequently ground thoroughly for 10 min using the mortar and pestle to ensure uniform mixing of the two components (Figure S1). The choice of 30 wt % glycerol was based on the fact that it is on a level that ensures efficient plasticization. (33) The mixture was then allowed to dry at room temperature (20 °C) for 4–5 h. After that, the material was again ground with the mortar and pestle to obtain a fine powder of the final protein/glycerol mixture. The particle size was 302 ± 241 μm, as obtained from scanning electron microscopy images. The powder was then subjected to compression molding in a Fontijne Press TP 400 (Delft, Netherlands) instrument at three different temperatures (110, 120, and 130 °C) and pressing times (5, 10, and 15 min) with a force of 250 kN. The choice of these conditions was based on previous work on protein materials. (34) Samples are named according to the pressing conditions, that is, SCP/Gly-X-Y, for example, SCP/Gly-110-10. The sample composition and pressing conditions are also summarized in Table S1. Circular molds of 10 cm diameter and 200 μm thickness were used for making the films.

2.3. Fourier-Transform Infrared Spectroscopy

Fourier-transform infrared spectroscopy (FTIR) of the films was performed in attenuated total reflection (ATR) mode on a PerkinElmer Spectrum 400 instrument equipped with a single-reflection ATR accessory Golden Gate crystal. Before the measurement, the films were thoroughly dried in a desiccator with silica gel for 7 days. The films were then mounted onto the crystal, and the spectra were recorded from 500 to 4000 cm–1 with 16 scans at a resolution of 4 cm–1. The obtained spectra were then modified in Spectrum 10.5.1 software to perform a baseline correction and deconvolution of the FTIR peaks with an enhancement factor (γ) of 2 and a smoothing filter of 70%. These parameters have been used successfully in previous works. (35) Then, the amide I spectral range of 1700 to 1586 cm–1 of the abovementioned baseline-corrected spectra were loaded into Origin 9.1 software, and the deconvoluted spectra were fitted with 10 Gaussian peaks with fixed wavelengths until the fits reached a stable minimum with an $R2 > 0.9992$

2.4 Measure the tensile strength

The thermal stability of the protein films was determined using thermogravimetric analysis (TGA) in a Mettler Toledo thermobalance (TGA/SDTA 851e, Switzerland) at a scanning rate of 10 °C/min in a nitrogen atmosphere (50 mL min–1) at a scanning rate of 10 °C/min in a nitrogen atmosphere (50 mL min–1). Samples weighing less than 5 mg were placed in aluminum oxide crucibles and fired to temperatures ranging from 30 to 600 °C.

2.5. Thermal Analysis

The thermal stability of the protein films was determined using thermogravimetric analysis (TGA) in a Mettler Toledo thermobalance (TGA/SDTA 851e, Switzerland) at a scanning rate of 10 °C/min in a

nitrogen atmosphere (50 mL min–1). The samples of ~5 mg in weight were placed in aluminum oxide crucibles and heated from 30 to 600 °C.

2.6. Scanning Electron Microscopy with Field Emission

A Hitachi S-4800 field emission scanning electron microscope was used to examine the surface and cross-sectional morphology of the films. Using conductive carbon tape, the film samples were attached to a field emission scanning electron microscope sample holder. Before scanning, the samples were coated with palladium/platinum for 30 seconds in an ultra-high-resolution sputter coater (model 208H).

2.7 Analysis of Water Vapor Transmission

The water vapor transmission rate (WVTR) of the films was determined using the ASTM E95 standard cup method (QTC Sheen permeability cups, surface area: 10 cm2, Article no. VF2200, Netherlands). The WVTR was determined using the desiccant method (50–0 percent RH gradient over the film), in which the exposed area of the films was lowered using aluminum masks (hole area: 10 cm2, MOCON Inc., USA) and sealed at the open mouth of test cups containing anhydrous silica gel as the desiccant. Before the tests, the films were conditioned for 24 hours at 23 1 °C and 50% relative humidity. Throughout the measurements, the cups were kept in a controlled humidity chamber (23 1 °C and 50% RH). At 30-minute intervals, the cups were weighed. Due to moisture absorption by the desiccant from the atmosphere, the mass gain of the cups was recorded, resulting in a plot of weight change versus time with a slope of 'n'. WVTR = (nl)/A was computed using the slope, sample thickness (l), and surface area (A). By dividing the WVTR by the pressure difference across the film, the water vapor permeability (WVP) was computed. The tests were carried out in triplicate.

2.8 Rate of Oxygen Transmission

A Mocon Ox-Tran Twin instrument was used to assess the oxygen permeability (OP) by ASTM D 3985-95. The films were sandwiched snugly between two aluminum foils with a 5 cm2 exposed film area, then fed into a diffusion cell and purged with nitrogen gas to measure any oxygen leakage from the instrument. Following the background measurements, the samples were exposed to oxygen (99.95%) on one side at 23 °C and 50% RH, and the oxygen transmission rate was standardized regarding film thickness and oxygen pressure to produce the OP. For most samples, two replicate measurements were taken.

2.9 Biodegradation in the soil

The ASTM D5988 standard, with minor adjustments, was used to test the biodegradability of the soil in a laboratory setting. Up to 8.2 months, biodegradability was monitored. The soil respiration trial consisted of 100 g of soil (1/3 agricultural land, 1/3 meadow, and 1/3 forest) in 1 L hermetically sealed flasks. After accounting for the CO2 release in the baseline test, the degradation of the polymers was monitored by measuring CO2 release in the flasks (soil as such). Because the total organic content (TOC) of the SCP materials and the home compostable bag were unknown, the test findings were stated in terms of VS content [VS = organic matter [volatile solid (VS)]]. The TOC of 45 percent was utilized to calculate biodegradability (which is the TOC of the starch used). Duplicates of the four samples (incubated at 33 °C) were used. Sample 1 had 4.5 g starch per kilogram of soil and 2 g carbon per kilogram of soil. Sample 2 had 3.1 g SCP/Gly-110-10, equating to 2.2 g VS per kilogram of soil. Sample 3 contained 3.1 g of

SCP/Gly-130-10, which equaled 2.2 g VS/kg soil. 3.0 g of a home compostable bag (supermarket Lidl, 40% biobased content, adhering to the norm NFT 51–100 and HOME OK compost label) was combined with about 3.0 g VS/kg soil in Sample 4. The starch was in the form of a fine powder, while the remaining samples were cut films

3. Results and discussions

3.1 General Film Appearance

The films were brownish, translucent, and flexible (Figure 1). Only a few single cells with intact cell walls could be observed with field emission scanning electron microscopy (Figure 2A), which then showed that the majority of the cells were disintegrated into a continuous medium/matrix, similar to the case of disintegrated cellulose pulp fibers in a grease-proof paper. (37) The cross-section images (Figure 2B) also show some intact cells. However, there is no special development in features with different processing temperatures.

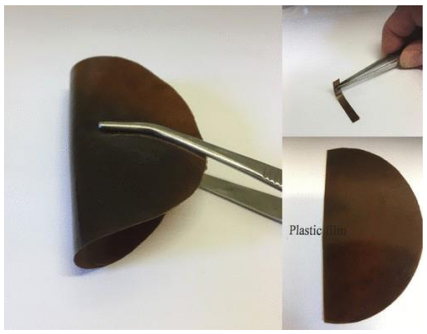

Figure 1

Figure 1. Flexibility and the color/translucency of the films (left: SCP/Gly-130-5, right two images: SCP/Gly-130-15).

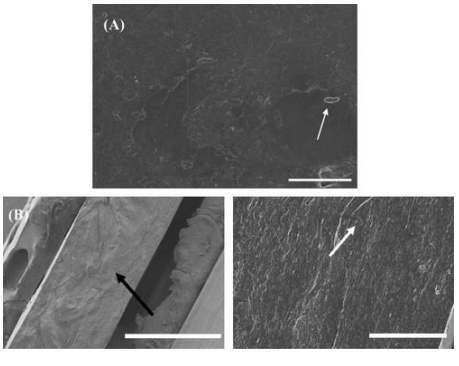

Figure 2

Figure 2. SEM images of (A) surface of the SCP/Gly-110-15 film (scale bar is 10 µm), and (B) cryofracture cross-section of SCP/Gly-130-5 film (scale bars are 300 and 20 µm for the left- and right-hand side

images, respectively). White arrows point at single cells, and black arrow points at the cross-section of the sample.

3.2Mechanical properties

Mechanically, the films appeared to be flexible, resembling polyethylene packing film (Figure 1). The different pressing conditions had no discernible effect on the overall appearance of the films. Packaging films' mechanical qualities are crucial because they represent the films' endurance during packing, handling, and storage. Figure 3 shows the tensile properties of the current protein films in terms of Young's modulus, tensile strength, extensibility, and toughness.

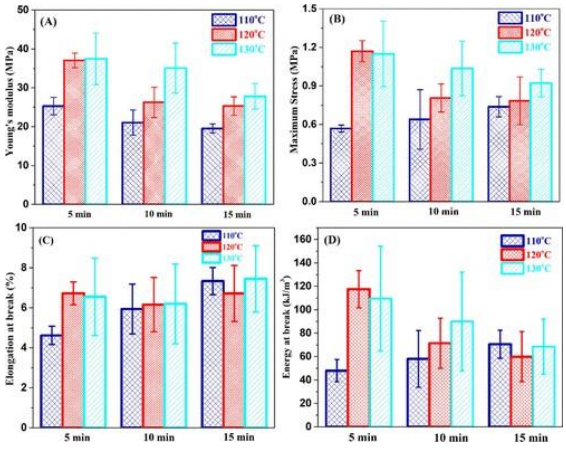

Figure 3

Figure 3. Tensile properties of all films at different pressing temperatures and times (A: stiffness, B: Maximum Stress, C: Extensibility, and D: Energy at break).

Because all the films had the same protein/glycerol ratio, the differences in their attributes were exclusively due to the processing parameters, such as pressing time and temperature. With increasing pressing temperature, all films' stiffness (Young's modulus) and strength (maximum stress) increased overall (independent of pressing time) (Figure 3). Considering all the pressing periods, the extensibility (percent elongation at break) and toughness (energy at break) showed a less obvious pattern. The mechanical qualities deteriorated with increasing pressing time, except for strength, extensibility, and toughness at 110 °C. Heat-induced aggregation, which is common in proteins, was responsible for the alterations as the temperature rose.

The declining pattern of the numbers over time, on the other hand, was most likely attributable to some degradation. It's difficult to predict whether processes will dominate the characteristics under a

specific pressing situation (heat-induced aggregation or thermal degradation/oxidation). The strength and stiffness were comparable to those of other glycerol-plasticized protein composites, but the ductility was low. (38)

3.3 Thermal Properties

The influence of pressing time and temperature on the thermal characteristics of the films was investigated using TGA. Figures S2 and 4 show the TGA and first-derivative curves, respectively. Similar to other proteins, all of the films showed a three-step weight loss profile. (39,40) The evaporation of moisture caused the initial weight to drop from 30 to around 150 °C. The weight loss in the second stage, between 150 and 250 °C, was mostly due to the loss of a glycerol plasticizer (glycerol's boiling point is 290 °C), and the weight loss in the third stage, between 250 and 400 °C, was due to the breakdown of the leftover material, which was high in protein. (39,40) The thermal stability of the films pressed at higher temperatures is marginally improved, and it is more clearly seen in the first-derivative plot for a longer time (Figure 4). This appeared because glycerol weight loss shifted to higher temperatures, implying that at higher temperatures and longer pressing times, intermolecular connections between glycerol and amino acid groups formed.

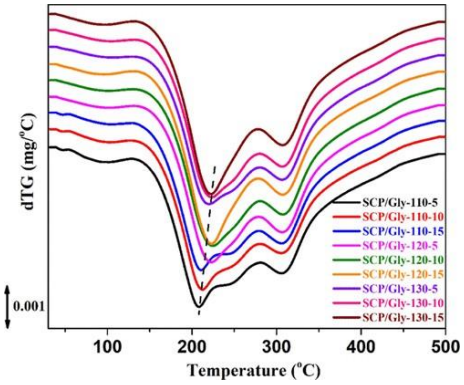

Figure 4

Figure 4. First derivative TGA plots of all films.

3.4. Permeability of Water Vapor

The WVP is an important feature of a food packaging material that influences food quality during preservation and storage because excessive moisture loss/gain via the packaging material can cause food quality to deteriorate and the shelf-life to be shortened. The WVP of protein-based films is determined by several inherent and external factors. (41) Amino acid composition (e.g., polar, and non-polar amino acid concentration), inhomogeneity, surface charge, pH, molecular size, and three-dimensional form are all intrinsic variables. When comparing the results in Table 1, keep in mind that as the plasticizer content rises, so does the permeability. Film processing conditions, temperature, and

relative humidity are all crucial extrinsic factors. the WVP of protein-based films is compared to synthetic polymers as shown in table 1

In comparison to synthetic polymers such as polyethylene, poly (vinylidene chloride), and polyester, protein-based films have poor water vapor barrier characteristics. This is owing to proteins' hydrophilic functional groups, which allow for greater water vapor molecule solubility and thus increased permeability. (42) Even with changes in relative humidity and plasticizer concentration, the WVPs of SCP-based films are comparable to or lower than those of other protein-based films, which is encouraging (Table 1). The significant amount of nonpolar amino acid moieties in SCP-based proteins is responsible for this (refer to the section on amino acid content below). Furthermore, the presence of lipids (the proteins are not defatted) in the film samples contributes to the matrix's hydrophobicity, which lowers water solubility. It's worth noting that the WVP values of the three protein films examined here were all similar (within the standard deviation). As a result, SCP-based films can be considered a low-cost and potential alternative to other plants/animal-based protein films, such as those used in food packaging.

Table 1. WVP of SCP/Gly Films in Comparison to Some Well-Known Protein Films and Synthetic Polymers

Sample[a]	Temp. (°C), RH gradient (%)	WVP (g mm m^{-2} h^{-1} kPa^{-1})
SCP/Gly-130-5	23, 0/50	0.46 ± 0.02
SCP/Gly-130-10	23, 0/50	0.47 ± 0.05
SCP/Gly-130-15	23, 0/50	0.48 ± 0.01
WPI/glycerol (70/30)*	25, 0/100	15.8
wheat gluten/glycerol (67.5/32.5)*	37.8, 0/49	1.27
gelatin/glycerol (80/20)*	25, 50/100	3.70
native WPI/Gly (70/30)	25, 0/71	5.06
heat denatured WPI/Gly (70/30)	25, 0/71	4.96
β-lactoglobulin/Gly (70/30)	25, 0/70	3.90 ± 0.29
corn zein/Gly (65/35)	0/97[b]	2.70
wheat gluten/Gly (75/25)	25, 0/75	0.64
sodium caseinate/Gly (47/53)	20, 0/45	0.47
poly(vinylidene chloride)	25, 0/100	0.0008
LDPE	28, 0/100	0.0013
polyester	25, 0/100	0.0070

All protein films were cast except those with a *, which were compression molded. WPI: whey protein isolate, LDPE: low-density polyethylene.

Temperature not disclosed.

3.5 Permeability to Oxygen

In general, protein-based films are good oxygen barriers in dry environments because they may build a large hydrogen bond network that prevents oxygen from flowing through. (51) This property is crucial when extending the shelf life of certain foods, such as high-fat foods that are known to oxidize and develop rancid off-flavors. Furthermore, oxygen may stimulate bacteria development. (52) The OP of the SCP/Gly films in Figure 5 can be compared to some protein-based films and synthetic polymers using Table 2 data. The table shows that there was no significant variation in OP of SCP-based films processed under various conditions, with values ranging from 175 to 205 cm3 m m–2 day–1 kPa–1 (Figure 5). The oxygen penetration through these films appears to be unaffected by changes in molecular structure (such as aggregation) as a function of pressing times and temperatures. At equal glycerol content, temperature, and relative humidity, the OP values of other protein-based films, such as whey protein isolate (WPI), -lactoglobulin, and WG, are slightly higher. (46,48,53) It's worth noting that the SCP/Gly films have a lower protein content and a higher lipid content than the other materials. As a result, by extracting the purified protein fraction from single cells for commercial applications, the OP might be improved even more. A continuous and broad hydrogen-bonded network is formed as the protein percentage is increased, which is one of the reasons for the low OP in protein-based films. Nonetheless, the SCP-based films, like other protein films, have significantly better OP barrier qualities than synthetic polymers like low/high-density polyethylene (LDPE and HDPE). (55) Because the processing conditions do not affect the OP, they can be tweaked to improve other attributes (such as toughness) without lowering the OP unintentionally.

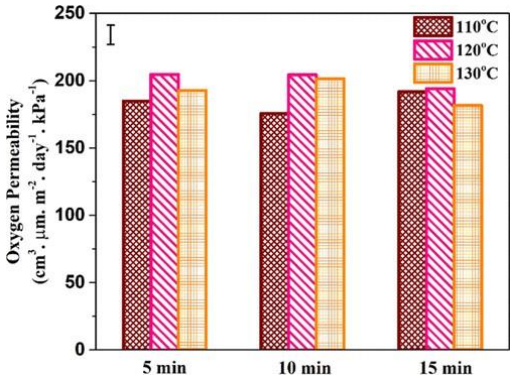

Figure 5

Figure 5. The oxygen permeability of all films

Table 2. Oxygen Permeability Values of Some Common Protein Films and Synthetic Polymers

Sample[a]	Conditions, Temp. (°C), RH gradient (%)	OP (cm^3 µm m^{-2} day^{-1}
β-lactoglobulin/Gly (70/30)	23, 0/40	25
(60/40)	37, 0/40	150 ± 2
wheat gluten/Gly (75/25)	25, 0/52	40 ± 1
wheat gluten/glycerol (75/25)*	23, 0/90	22−30
CO_2-casein/Gly (70/30)	23, 0/50	144
unhydrolyzed WPI/Gly (3/1−0.8/1)	23, 0/50	41−333
hydrolyzed WPI/Gly (5.5% DH)[b] (3/1−0.8/1)	23, 0/50	42−112
LDPE	23, 0/50	1870
HDPE	23, 0/50	427
polyester	23, 0/50	15.6
EVOH (70% VOH)	23, 0/50	0.1
EVOH (70% VOH)	23, 0/95	12

All protein films were cast except that with a *, which was compression molded. WPI: whey protein isolate, LDPE: low-density polyethylene, HDPE: high-density polyethylene, EVOH: Poly(ethylene-co-vinyl alcohol), VOH: vinyl alcohol.

DH represents the degree of hydrolysis.

3.6 Amino Acid Content and Protein Conformation

FTIR spectroscopy was used to investigate the secondary structure of the neat and plasticized SCP films. The stretching carbonyl vibration in the amide group causes the amide I band area from 1590 to 1700 cm–1 to be typical of the secondary protein structure. (56,57) Tables S2 and S3 summarize the origin of the peaks, their positions and assignments, and relative sizes under various pressing conditions. Figure 6 shows the deconvoluted and resolved FTIR spectra of the pure protein powder and the plasticized films. The relative peak areas of the films made at different temperatures and for different durations of time showed no significant differences. However, as compared to the protein powder, there was a significant variation in the relative band areas of all the films, showing the role of thermal treatment on protein secondary structure. The difference in the extent of the IR absorption in the low wavenumber range (peak locations between 1610 and 1625 cm–1), which is attributed to the contribution from highly hydrogen-bonded ß-sheets, is the most notable feature. Protein aggregation is indicated by an increase

in this sort of -sheet, (36) and thus the IR measurements revealed that protein aggregation occurred during pressing. (35) This could explain why at higher pressing temperatures, overall stiffness and strength rise (Figure 3). Aggregation is a process in which a protein material's cohesiveness is increased. Apart from the strong hydrogen bonding caused by -sheet formation, the reformation of disulfide cross-links, as seen in other cysteine-containing proteins like WG and whey, may have also contributed to the aggregated structure. (36,58,59) The SCP protein, on the other hand, has a low cysteine concentration (Table 3). Biopeptide bonds, which can form at high temperatures, for example, may also contribute to aggregation. (60) These mainly involve lysine, which is present in lower concentrations in soy protein isolates and egg white compared to whey. It's also higher than in WG (61). By generating dityrosine cross-links, tyrosine can aid in aggregation. The amount of tyrosine in this product is comparable to that of egg white. (61) It's worth noting that the high concentration of alanine and glycine with tiny side groups aids in protein chain packing. It's also worth noting that the SCP protein has a particularly hydrophobic nature due to its large amount (about 50%) of hydrophobic amino acids (62) (much greater than WG and whey (61)). The protein, however, is still hydrophilic when compared to other hydrophobic polymers.

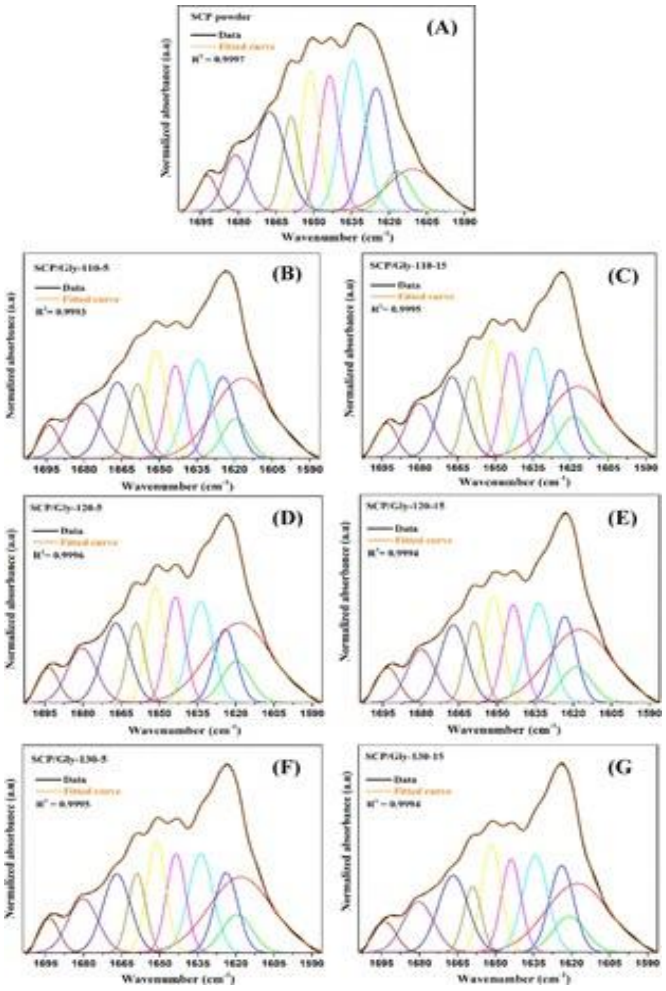

Figure 6

Figure 6. Fourier-deconvoluted infrared spectra (ATR) of amide I band of (A) SCP powder, and of SCP/Gly film (B) 110-5, (C) 110-15, (D) 120-5, (E) 120-15, (F) 130-5, and (G) 130-15 samples.

Table 3. Amino Acid Profile of the SCP

Amino acid	Wt % of total protein content
cysteineb	0.9
methionineb	1.9
valineb	7.3
isoleucineb	4.9
leucineb	8.2
tyrosineb	4.0
phenylalanineb	4.9
lysine	5.6
histidine	2.0
arginine	6.3
aspartic acid/asparagine	9.6
threonine	5.2
serine	3.4
glutamic acid/glutamine	12.2
prolineb	5.1
glycineb	7.6
alanineb	9.1
tryptophanb	1.9

3.7 Biodegradation

In the first month of incubation, the soil respiration rate (baseline) was 18 mg C (kg soil)1 day–1, showing that the soil employed in the experiments had high microbial activity. The average soil respiration rate was 11–14 mg C (kg soil)1 day–1 in the second and third months of incubation, and 7 mg C (kg soil)1 day–1 in the last two periods (3 to 6 months and 6 to 8.4 months). In all cases, the substrates (polymers) degraded within the first three months. The degradation of the polymers, as well as the starch in the positive control, essentially stopped between 3 and 6 months of incubation. The pH of the soil at that time (6 months incubation) was determined to be 4.8–5.2 in all situations. Such a pH is unfavorable, and it may explain (in part) why polymer breakdown halted at that point. When the sample surface reaches a high degree of oxidation (saturation), it is common to see a significant fall in the

biodegradation rate. The experiment can then be ended according to the standard. The experiment was, nevertheless, continued here. After 6 months of incubation, the soil pH was adjusted (with a phosphate buffer) in all situations. Even though the soil was still active (11–14 mg C (kg soil)1 day–1) after 6–8 months, no further deterioration was found for any of the samples As a result, the majority of the deterioration happened in the first three months, and the degradation rate "profiles" for all samples were identical. For the starch sample, total carbon respiration after 3 months was 660 mg C (kg soil), or 15% on a VS basis (32 percent of the added carbon) (Table 4). The figure for the SCP/Gly-110-10 sample was 206 mg C (kg soil)1, or 9% VS (assuming 45 percent TOC, the deterioration after 3 months of incubation was expected to be 20%). The SCP/Gly-130-10 samples had comparable results to the SCP/Gly-110-10 sample (Table 4). The rate of decomposition for the home compostable bag was slightly lower than for the protein samples. The fine starch powder had a greater accessible surface area, which resulted in a faster starch breakdown.

Table 4. Soil Biodegradation Data after 3 Months

Material	mg C (kg soil)$^{-1}$[a]	Degradation (%)[b]	Degradation (%)[c]
SCP/Gly-110-10	206 ± 9	9.1 ± 0.4	20.3 ± 0.9
SCP/Gly-130-10	214 ± 16	9.6 ± 0.7	21.2± 1.6
compostable bag	223 ± 14	7.4 ± 0.5	16.7± 1.0
Starch	660 ± 44	14.5 ± 1.0	32.3 ± 2.1

Total carbon respiration.
Total carbon respiration in % of VS basis.
Same as in b but calculated based on a TOC of 45%.

4. Conclusion

A novel type of protein-based plastic has been generated using single cells cultured from potato trash, as described in this article. Compression molding was used to create the films, which were pressed at three distinct temperatures and periods. In all the thermally treated films, FTIR analysis confirmed protein denaturation and aggregation formation. The mechanical properties of all the films were altered by the pressing duration and temperature, with tensile strength and Young's modulus increasing with pressing temperatures from 110 to 130 °C due to network strengthening via aggregate formation (increases the material cohesion). However, as the pressing duration was increased, the strength and modulus decreased, indicating protein breakdown.

TGA found that films pressed at higher temperatures and for longer periods had improved thermal stability from 200 to 250 °C, suggesting interactions between glycerol and amino acids at high temperatures. While the films' WVP was comparable to or better than other protein films, the OP values were slightly higher and might be enhanced further by increasing the protein proportion of the films (a material with high protein content will have an extensive hydrogen-bonded network, which reduces O2

permeation). The OP values, on the other hand, were much higher than those of commonly used plastic packaging materials like LDPE and HDPE. The degradability of the SCP materials was comparable to that of a biodegradable bag used in the home.

Protein materials have the advantage of not causing the same difficulties as microplastics do. They are not persistent, yet they provide sustenance to both plants and animals. The combined findings show that SCP-based bioplastic films have the potential to be a sustainable alternative to environmentally harmful plant/animal-protein-derived goods, other biopolymeric films (polysaccharides), and synthetic polymers in applications such as packaging. SCPs could potentially be made from solid food wastes in the future, which is a growing study field for bioplastics development. (63) They, like other proteins, must be protected from excessive moisture during storage.

References

(1) Assad, I.; Bhat, S. U.; Gani, A.; Shah, A. Protein Based Packaging of Plant Origin: Fabrication, Properties, Recent Advances and Future Perspectives. Int. J. Biol. Macromol. 2020, 164, 707−716.

(2) Bourtoom, T. Edible Films and Coatings: Characteristics and Properties. Int. Food Res. J. 2008, 15, 237−248.

(3) Chiralt, A.; González-Martínez, C.; Vargas, M.; Atarés, L. Edible films and coatings from proteins, In Proteins in Food Processing, 2nd Ed.; Woodhead Publishing Ltd: U.K., 2018; pp 477−500.

(4) Vicente, A. A.; Cerqueira, M. A.; Hilliou, L.; Rocha, C. M. R. Protein-based resins for food packaging. Multifunctional and Nanoreinforced Polymers for Food Packaging; Woodhead Publishing Ltd: U.K., 2011, pp 610−648.

(5) Krochta, J. M. Proteins as Raw Materials for Films and Coatings: Definitions, Current Status, and Opportunities. Protein Based Films and Coatings; CRC Press: Boca Raton, FL, 2002; pp 1−42. 9781587161070.

(6) Dubey, N. K.; Dubey, R. Edible films and coatings: An update on recent advances. Biopolymer-Based Formulations; Elsevier: Netherlands, 2020, pp 675−695. DOI: 10.1016/B978-0-12-816897-4.00027- 8.

(7) Mohamed, S. A. A.; El-Sakhawy, M.; El-Sakhawy, M. A.-M. Polysaccharides, Protein and Lipid Based Natural Edible Films in Food Packaging: A Review. Carbohydr. Polym. 2020, 238, 116178.

(8) Kouhi, M.; Prabhakaran, M. P.; Ramakrishna, S. Edible Polymers: An Insight into Its Application in Food, Biomedicine and Cosmetics. Trends Food Sci. Technol. 2020, 103, 248−263.

(9) Matassa, S.; Batstone, D. J.; Hülsen, T.; Schnoor, J.; Verstraete, W. Can Direct Conversion of Used Nitrogen to New Feed and Protein Help Feed the World ? Environ. Sci. Technol. 2015, 49, 5247− 5254.

(10) Ezeh, A. C.; Bongaarts, J.; Mberu, B. Global Population Trends and Policy Options. Lancet 2012, 380, 142−148.

(11) Anupama; Ravindra, P. Value-Added Food: Single Cell Protein. Biotechnol. Adv. 2000, 18, 459−479.

(12) Sharif, M.; Zafar, M. H.; Aqib, A. I.; Saeed, M.; Farag, M. R.; Alagawany, M. Single Cell Protein: Sources, Mechanism of Production, Nutritional Value and Its Uses in Aquaculture Nutrition. Aquaculture 2021, 531, 735885.

(13) Matassa, S.; Papirio, S.; Pikaar, I.; Hülsen, T.; Leijenhorst, E.; Esposito, G.; Pirozzi, F.; Verstraete, W. Upcycling of Biowaste Carbon and Nutrients in Line with Consumer Confidence: The 'Full-Gas' Route to Single Cell Protein. Green Chem. 2020, 22, 4912−4929.

(14) García-Garibay, M.; Gómez-Ruiz, L.; Cruz-Guerrero, A. E.; Bárzana, E. Single Cell Protein, Yeasts and Bacteria. In Encyclopedia of Food Microbiology, 2nd Ed.; Elsevier: Netherlands, 2014; pp 431−438.

(15) Hülsen, T.; Hsieh, K.; Lu, Y.; Tait, S.; Batstone, D. J. Simultaneous Treatment and Single Cell Protein Production from Agri-Industrial Wastewaters Using Purple Phototrophic Bacteria or Microalgae − A Comparison. Bioresour. Technol. 2018, 254, 214−223.

(16) Matassa, S.; Boon, N.; Verstraete, W. Resource Recovery from Used Water: The Manufacturing Abilities of Hydrogen-Oxidizing Bacteria. Water Res. 2015, 68, 467−478.

(17) Ulber, R.; Sell, D.; Hirth, T. Renewable Raw Materials: New Feedstocks for the Chemical Industry; Wiley-VCH Verlag GmbH & Co. KGaA: Wienheim, Germany, 2011. ISBN: 978-3-527-63420-0

(18) Pikaar, I.; Matassa, S.; Rabaey, K.; Bodirsky, B. L.; Popp, A.; Herrero, M.; Verstraete, W. Microbes and the Next Nitrogen Revolution. Environ. Sci. Technol. 2017, 51, 7297−7303.

(19) Pikaar, I.; Matassa, S.; Bodirsky, B. L.; Weindl, I.; Humpenöder, F.; Rabaey, K.; Boon, N.; Bruschi, M.; Yuan, Z.; van Zanten, H.; Herrero, M.; Verstraete, W.; Popp, A.; Popp, A. Decoupling Livestock from Land Use through Industrial Feed Production Pathways. Environ. Sci. Technol. 2018, 52, 7351−7359.

(20) Nasseri, A. T.; Rasoul-Ami, S.; Morowvat, M. H.; Ghasemi, Y. Single Cell Protein: Production and Process. Am. J. Food Technol. 2011, 6, 103−116.